J. Astron. Space Sci. 25(4), 347–360 (2008)

Development of a Hardware-In-Loop (HIL) Simulator for Spacecraft Attitude Control Using Momentum Wheels

Dohee Kim[1], Sang-Young Park[1†], Jong-Woo Kim[2], and Kyu-Hong Choi[1]

[1]Astrodynamics and Control Lab., Dept. of Astronomy, Yonsei University, Seoul 120-749, Korea

[2]Mechatronics & Manufacturing Technology Center, Samsung Electronics Co., Suwon 443-742, Korea

email: spark@galaxy.yonsei.ac.kr

(Received October 10, 2008; Accepted November 18, 2008)

Abstract

In this paper, a Hardware-In-the-Loop simulator to simulate attitude control of spacecraft using momentum wheels is developed. The simulator consists of a spherical air bearing system allowing rotation and tilt in all three axes, three momentum wheels for actuation, and an AHRS (Attitude Heading Reference System). The simulator processes various types of data in PC104 and wirelessly communicates with a host PC using TCP/IP protocol. A simple low-cost momentum wheel assembly set and its drive electronics are also developed. Several experiments are performed to test the performance of the momentum wheels. For the control performance test of the simulator, a PID controller is implemented. The results of experimental demonstrations confirm the feasibility and validity of the Hardware-In-the-Loop simulator developed in the current study.

Keywords: attitude control, hardware-in-the-loop simulator, momentum wheels, testbed

1. Introduction

Embedded systems are designed to control complex plants such as land vehicles, spacecrafts, Unmanned Aerial Vehicles (UAVs), aircrafts, weapon systems, marine vehicles, and jet engines. They generally require a high level of complexity within the embedded system to properly manage the complicated plant under control (Edwards et al. 1997). A Hardware-In- the-Loop (HIL) simulation is a technique that is used increasingly in the development and test of complex real-time embedded systems. In particular, for duplicating spacecraft attitudes as the representative of complex real-time embedded systems, it is necessary to develop an HIL simulator for spacecraft attitude control. However, it is true that the current trend in the research area of attitude control development is missing the significant step of validating theoretical results with experiments using a hardware simulator (Kim et al. 2001). Experimental testing using a hardware simulator is very effective in verifying control laws before they are incorporated in the future generation of spacecraft; however, the greatest difficulty in implementing spacecraft control laws is overcoming a one-g environment, whereas the real spacecraft operate in a zero-g environment. The air-bearing system makes it possible to reproduce an environment that is similar to the zero-g in space. Pressurized air

†corresponding author

passes through small holes, and then the air makes the hemi-spherical bearing float the moving part as it forms thin air-film. In addition, the moving part, a Hardware-In-the-Loop (HIL) simulator, can implement diverse types of control schemes and identify attitude dynamics in that it is composed of subsystems with a similar complexity to that of the actual spacecraft (Schwartz et al. 2003). In other words, not only is a similar torque-free environment to the space environment created through the air-bearing system, but also the actual spacecraft is duplicated through the HIL simulator connected to the air-bearing system. Many previous studies have been done to develop HIL systems (Schwartz et al. 2003, Wang et al. 2006).

The main objective of the current research is to develop an HIL simulator for spacecraft attitude control using momentum wheels. The HIL simulator will enhance the reliability of micro-satellites and help in the accumulation of satellite development technology. The HIL simulator developed in this research can reproduce spacecraft attitudes in a space environment using the table-top air-bearing system displaying the degree of freedom of both +/–180 in the yaw axis and +/–45 in the roll and pitch axes. The mass of the HIL simulator is about 50 kg. In addition, synchronizing with three momentum wheels and an AHRS (Attitude Heading Reference System) sensor, the HIL simulator can perform 3-axis control through the signal interface between the AHRS and three momentum wheels. Moreover, for wireless communication similar to that of real spacecraft in a space environment, it uses TCP/IP communication with a wireless network router and a wireless LAN card. Three sealed lead storage battery sets (total 6 batteries) can also supply on-board power for each system module, such as the momentum wheels, sensors, and PC104. Finally, MATLAB xPCtarget and Real-time workshop allow the simulator to perform real-time control to establish the environment of real time operation for the target PC. The HIL simulator developed in this research will contribute to the development of advanced technologies for spacecraft, and support for the verification of algorithms for attitude determination and control.

2. Requirements and Settings

2.1 Requirements

To develop an HIL simulator for a micro-satellite application use, the HIL simulator has the requirements listed in Table 1. It is essential to duplicate the torque-free environment of space with a spherical air bearing system. In addition, to test the performance of a micro-satellite, the HIL simulator needs to have a mass between 50 kg and 100 kg, as well as a 3-axis actuator and control system.

For the purpose of testing micro-satellites with various types of payloads in near future, both accuracy and slew rate specifications are given wide ranges. Power will have a maximum of 150 W/hr, that can cover the power needed during the eclipse period of a low orbit. The general orbital period of satellites in a low earth orbit is 95 $\sim$ 105 minutes. Furthermore, on the basis of satellites in a space environment, it is natural to consider wireless communication and a real-time operating system. The HIL simulator in this research receives wireless commands from the host PC and processes data in real time using the xPC target (MATHWORKS) for rapid prototyping. AHRS, as a 3-axis gyro sensor, senses the motion of the simulator for the attitude control of the HIL simulator. The attitude data are then processed in the PC104 computer (which is called the target PC), and they are transmitted to three momentum wheel assemblies. The application code, including operation and control, is developed on a desktop host PC before being downloaded onto the target PC.

Table 1. Requirements of HIL simulator for spacecraft attitude control.

Requirement factors	Data	Note
Environment	1g (gravity)	Low-torque environment
Mass	50~100 kg	On the level of micro-satellite
Control mode	3-axis control	3 momentum wheel assemblies
Accuracy	+/- 0.1deg ~ +/- 1deg	
Slew rate	0.05 deg/s ~ 0.5 deg/s	
Power	150 W/hr	On-board power system
Communication type	Wireless communication	
Operating system	Real-Time operating system	

2.2 Hardware settings

2.2.1 Air-bearing System

The air-bearing system produced by Specialty Components, INC [1] is chosen so that the system can replicate a space environment. The system used in this simulator can uphold up to 110kg with 652.93 kPa (80 psig). It is possible to maneuver +/–45 deg in the roll and pitch axes and +/–180 deg in the yaw axis.

2.2.2 Sensor and Actuator

The selected inertial subsystem provides attitude and heading measurements with static and dynamic accuracy that exceeds traditional spinning mass vertical and directional gyros. AHRS displays the static accuracy at less than +/–0.75 deg and the resolution at less than 0.1 deg so that it satisfies the requirements of attitude knowledge in Table 1.

Furthermore, the MTi sensor for post analysis provides the proper resolution and range using a sensor fusion algorithm (http://www.cadden.fr/documentations/MTi.pdf), which can integrate the roles of the MTi sensor such as the gyroscope, accelerometer, and magnetometer. Momentum Wheel Assembly (MWA) needs 3 sets for 3 axis control as seen in Figure 1, and is determined considering slew rate and maximum power. The motor for the customized MWA uses 12V and 4A (maximum continuous current) and can reach up to 5,500 rpm. Therefore, based on the mass properties of the wheel, it can adjust the amount of torque generated.

2.2.3 Power System

Since the HIL simulator for spacecraft attitude control duplicates the attitude of micro-satellites during the eclipse period, the on-board battery of the HIL simulator needs the supply of power during the eclipse period. Generally, the orbital period of the micro-satellites in low-earth orbit ranges from 95 min. to 105 min. In this period, assuming that the eclipse period is more than 50 % of the period, the power system should have a performance that can maintain the maximum consumption of power for each module during the period. Hence, the power system of the HIL simulator is designed so that the on-board power system of the simulator remains available in full operation for a maximum of 1 hour. The simulator uses three sealed lead storage battery sets (total 6 batteries, each battery set: 12V, 10Ah) as a main power supplier, which allows it to generate the power supply. In addition, in order to avoid data loss by sudden battery discharge, an on-board Unregulated Power Supply (UPS) and re-charger are used for the PC104.

2.2.4 Communication System

Basically, satellites need a wireless strategy for communication with the ground station. In

[1] http://www.specialtycomponents.com/nf/spherical.htm

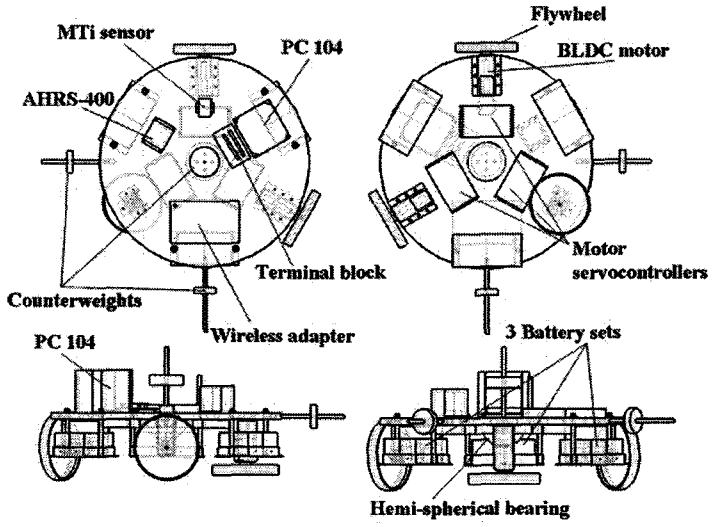

Figure 1. Four views of the HIL simulator for spacecraft attitude control (upper-left: top view, upper-right: bottom view, lower-left: side view, lower-right: another side view).

order to duplicate a satellite in the space environment, it is essential to establish a wireless network for the HIL simulator. For communication between the target PC (the embedded PC of the HIL simulator) and the host PC (a general desktop PC), TCP/IP communication is used. In order to establish TCP/IP communication, a wireless router is loaded on the platform of the simulator and a wireless USB adapter is used for the host PC.

2.2.5 Real-time and Embedded System

The HIL simulator uses a PC104 to process data and perform real-time control. Real-time and embedded system operates in constrained environments. These environments are on-board memory, processing power, speed, and timing constraints, which dictate the use of real-time operating systems in embedded software. The onboard PC104 computer consists of an Athena CPU, DMM-32x-AT (Data acquisition board), Emerald (Serial communication board), HESC104 (Re-charger & DC-DC converter), and BAT104 (Unregulated Power System) provided by Diamond Systems Corp.

2.3 Software Setting

The HIL simulator needs real-time operations in a wireless environment in that the simulator reflects a micro-satellite in the space environment. In order to establish such an environment, the HIL simulator uses an xPC target and the Real-Time Workshop of MATLAB. The xPC target can operate the HIL simulator totally, control several I/O boards in the simulator, and give the simulator various commands through the host PC. In addition, in the target PC, the xPC target enables the simulator to embody a real-time environment as a loading real-time kernel that controls the CPU of the target PC and provides a wireless interface using TCP/IP communication between the target PC and the host PC. In addition, Real-Time Workshop functions to transform SIMULINK code for xPC target applications into C code when downloading. The HIL simulator uses the Real-Time Workshop Embedded Coder, which provides it with the embedded real-time target designed for customization

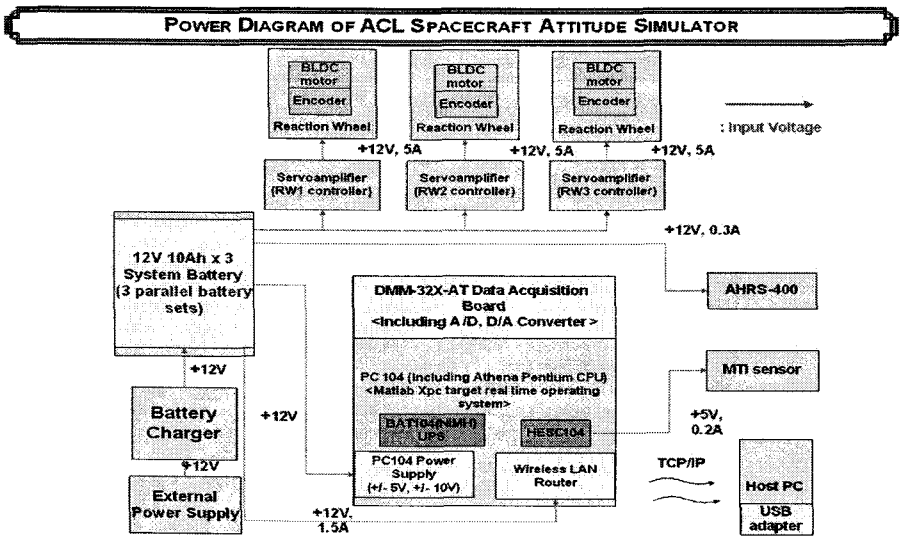

Figure 2. Power diagram of the HIL simulator.

and generates the code in embedded C format, a compact format designed for production code generation. The host PC has MATLAB, SIMULINK, and the Real-Time Workshop. Using the build tools on the host, the code and an executable program that runs on the target system are created.

3. Interfaces

3.1 Power Interface

As soon as an HIL simulator is connected to the on-board power system (3 battery sets), the simulator begins to fulfill commands from host PC. Figure 2 shows the entire power flow supplied by the three battery sets (12V, 10Ah). Specific functions are assigned to each battery set. The location of each battery set is shown in Figure 1. The first battery set supplies power source to one momentum wheel assembly and a dc-dc converter of the PC104.

Through the additional channel of the dc-dc converter, the 5V power source is supplied to the MTi sensor. Next, the second battery set takes charge of the power of another momentum wheel assembly (motor servo controller and brushless dc motor) and wireless network router. Finally, the third battery set is responsible only for the other assembly.

3.2 Signal Interface

An HIL simulator can reproduce the attitude control of the micro-satellite through the harmonious interface of the total system. While the simulator performs a control algorithm downloaded from a host PC, attitude sensors measure the attitude variations, which are analog signals with information about the angular rates and angular accelerations of the 3 axes. The changed attitude allows the momentum wheel assemblies to be repeatedly actuated to the desired orientation. The entire signal flow of the HIL simulator is shown in Figure 3. As seen in Figure 3, the attitude sensors

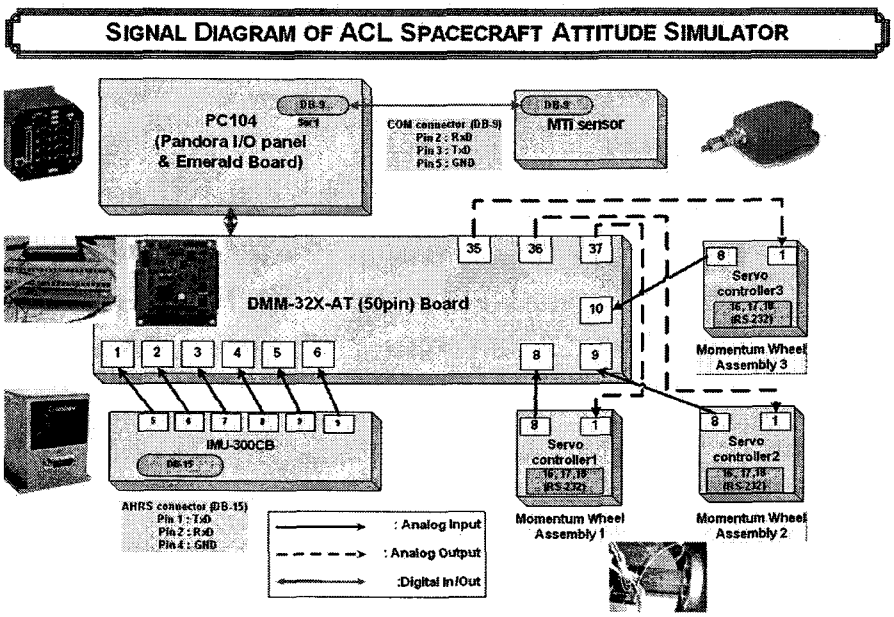

Figure 3. Signal diagram of the HIL simulator.

receive attitude information and then the attitude data (Roll, Pitch, Yaw angular rate) of AHRS are transferred to the data acquisition board in analog form. After then, according to the control algorithm downloaded to flash memory, the CPU of the target PC processes the acquired attitude data and operates the momentum wheels to move to the desired orientation.

4. Estimation of the Inertial Matrix of the HIL Simulator

4.1 Equations of Motion

Initially, for the purposes of designing the HIL simulator, a CAD program such as SolidWorks is used. The value of the moment of inertia (MOI) produced through this CAD program is utilized for some experiments. The value should be estimated through the proper algorithms. Therefore, for the estimation of the MOI of the simulator, a 3-2-1 Euler angle sequence is used to describe the attitude of the HIL simulator and equations of motion for the simulator are established. The coordinates of the HIL simulator are described in Fig. 4. The HIL simulator for attitude control is made up of four rigid bodies such as a platform (simulator's body) and three momentum wheels. The angular momentum consists of the angular momentum of simulator's body (i.e., the entire simulator except for the three wheels) and the angular momentums of the three wheels. The equation of motion is shown in eq. (1) for an HIL simulator from Euler's equations, where there is no control torque (Kim 2008).

$$(mg\vec{r}_M) \times \vec{K} = I^{I}\dot{\omega}^{I\to B} + {}^{I\to B}\omega \times I\,{}^{I\to B}\omega + \sum_{i=1}^{3}\left(I^{i}\,{}^{B}\dot{\omega}^{B\to w_i} + {}^{I\to B}\omega \times I^{i}\,{}^{B\to w_i}\omega\right) \qquad (1)$$

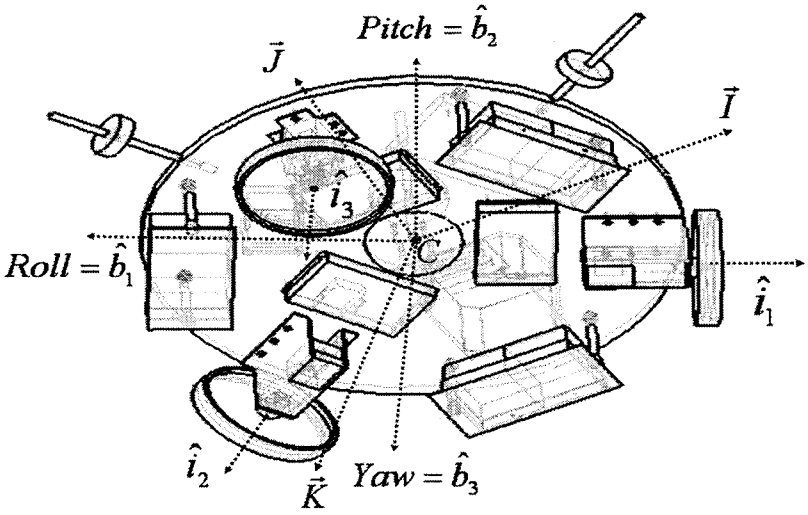

Figure 4. Definition of coordinates (I, J, K: inertial coordinate, b1, b2, b3: body fixed coordinate, i_1, i_2, i_3: three wheel axes).

The left side of the equation represents the total torque generated by external force. $\vec{r}_M$ is the position vector from the center of bearing to the center of gravity. $\vec{K}$ is the unit vector in the inertial frame directed to the center of the Earth. The right side of the equation refers to the rate of angular momentum change of the HIL simulator. I^I is the inertial moment of simulator's body, $\overset{I\to B}{\omega}$ is the angular velocity of the simulator's body with respect to the inertial coordinate, I^i is the inertial moment of each wheel, and $\overset{B\to w_i}{\omega}$ is the angular velocity of each wheel with respect to the simulator's body (i.e., the body fixed coordinate). The dot $(\cdot)$ represents a differential with respective time.

4.2 Least-square algorithm for the estimation of the inertial matrix

Now, on the basis of the coordinates and the equation of motion for the HIL simulator mentioned in previous sub-section, the estimation scheme of the inertial matrix is discussed. The HIL simulator performs a torque control by inserting input acceleration into the momentum wheel. The torque caused by gravity is only an external disturbance torque because other torques such as aerodynamic torque and various friction torques are considered very small. Therefore, gravity solely affects the moment of inertia of the simulator. In this respect, a least-squares algorithm with the regression form shown in eq. (2) can be utilized to estimate the inertia matrix (Tanygin & Williams 1997).

$$[A]\{x\} = \{T\} \tag{2}$$

With a view to utilizing the least-squares algorithm, it is essential to change eq. (1) into the regression form, like in eq. (2). For this work, we need to transform the frame of the wheels into the body frame of the HIL simulator. Using the coordinates in Figure 4, these coordinate transformations can be obtained. Finally, $[A]$, $\{x\}$, and $\{T\}$ of eq. (2) are given by

$$[A] = \begin{bmatrix} \dot{\omega}_r & \dot{\omega}_p - \omega_r\omega_y & \omega_r\omega_p + \dot{\omega}_y & -\omega_p\omega_y & \omega_p^2 - \omega_y^2 & \omega_p\omega_y & 0 & \cos\phi\cos\theta & -\sin\phi\cos\theta \\ \omega_r\omega_y & \dot{\omega}_r + \omega_p\omega_y & \omega_y^2 - \omega_r^2 & \dot{\omega}_p & \dot{\omega}_y - \omega_r\omega_p & -\omega_r\omega_y & \cos\phi\cos\theta & 0 & -\sin\theta \\ -\omega_r\omega_p & \omega_r^2 - \omega_p^2 & \dot{\omega}_r - \omega_p\omega_y & \omega_r\omega_p & \dot{\omega}_p + \omega_r\omega_y & \dot{\omega}_y & \sin\phi\cos\theta & -\sin\theta & 0 \end{bmatrix}$$

$$\{x\} = [I_{xx} \quad I_{xy} \quad I_{xz} \quad I_{yy} \quad I_{yz} \quad I_{zz} \quad mgr_{Mx} \quad mgr_{My} \quad mgr_{Mz}]^T \tag{3}$$

$$\{T\} = \begin{Bmatrix} -I_{11}^{w_1}\dot{\omega}_1 + \frac{1}{2}I_{11}^{w_2}\dot{\omega}_2 \\ \frac{\sqrt{3}}{2}I_{11}^{w_2}\dot{\omega}_2 \\ I_{11}^{w_3}\dot{\omega}_3 \end{Bmatrix} - \begin{bmatrix} 0 & -\omega_y & \omega_p \\ -\omega_y & 0 & -\omega_r \\ -\omega_p & \omega_r & 0 \end{bmatrix} \begin{Bmatrix} -I_{11}^{w_1}\omega_1 + \frac{1}{2}I_{11}^{w_2}\omega_2 \\ \frac{\sqrt{3}}{2}I_{11}^{w_2}\omega_2 \\ I_{11}^{w_3}\omega_3 \end{Bmatrix}$$

where ϕ is roll angle, θ is pitch angle, ψ is yaw angle, $\omega_r, \omega_p, \omega_y$ are angular velocities of roll, pitch, and yaw axes in body frame, ω_i is the angular velocity of the i-th wheel with respect to the body coordinate,$I_{xx}, I_{xy}, I_{xz}, I_{yy}, I_{yz}, I_{zz}$ are the components of the moment of inertia of the simulator, I_{11}^{wi} is the first diagonal component of the moment of inertia for the i-th wheel. In the end, the estimation scheme of the inertial matrix in the components of $\{x\}$ using the least square estimation is as follows.

$$\{x\}_n = [A]_n^+\{T\}_n \tag{4}$$

where $[A]_n^+$ is the pseudo-inverse of $[A]_n$, and the subscript n denotes the th time step. In order to experimentally estimate the moment of inertia of the HIL simulator, ten experiments are done and a Proportional-Integral-Derivative (PID) type controller is implemented. For the estimation scheme, least-square algorithm, both angular velocity and angular acceleration of the simulator and momentum wheel are used to calculate $[A]_n$ and $\{T\}_n \cdot [A]_n^+$ is obtained by the computation of the pseudo-inverse using equation (5).

$$A^+ = \lim_{\delta \to 0}(A^*A + \delta I)^{-1}A^* \tag{5}$$

where A^* is the conjugate transpose of a matrix, A. For matrices whose elements are real numbers instead of complex numbers, $A^* = A^T$ (Penrose 1955).

4.3 Test results for the estimation of the inertial matrix

On the basis of the estimation algorithm in sub-section 4.2, the moment of inertia and the product of inertia obtained by 10 experiments are shown in Figures 5 and 6, respectively. The experiments estimate the inertia matrix of the HIL simulator:

$$I_{sim\_exp} = \begin{bmatrix} 1.926 & -0.015 & 0.012 \\ -0.015 & 1.988 & 0.016 \\ 0.012 & 0.016 & 3,590 \end{bmatrix} kg \cdot m^2 \tag{6}$$

The standard deviations of inertia matrix are as follows: $\sigma(\mathrm{I_{xx}}) = 0.00549$, $\sigma(\mathrm{I_{yy}}) = 0.00710$, $\sigma(\mathrm{I_{zz}}) = 0.00560$, $\sigma(\mathrm{I_{xy}}) = 0.00203$, $\sigma(\mathrm{I_{xz}}) = 0.00298$, $\sigma(\mathrm{I_{yz}}) = 0.00302$.

5. Design of Momentum Wheels

The ACL (Astrodynamics and Control Laboratory)'s HIL simulator for spacecraft attitude control uses three momentum wheel assemblies as its actuators in order to maneuver the simulator into

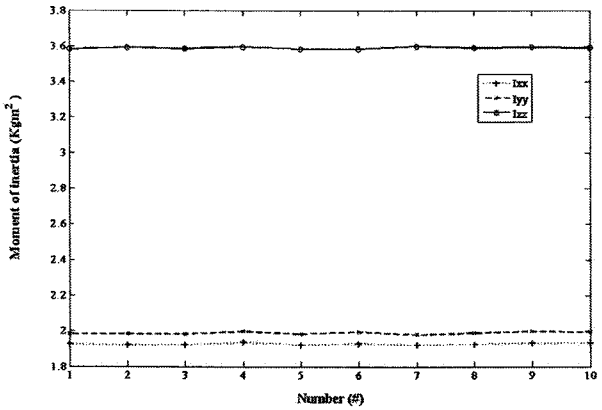

Figure 5. Moment of inertia by experiments.

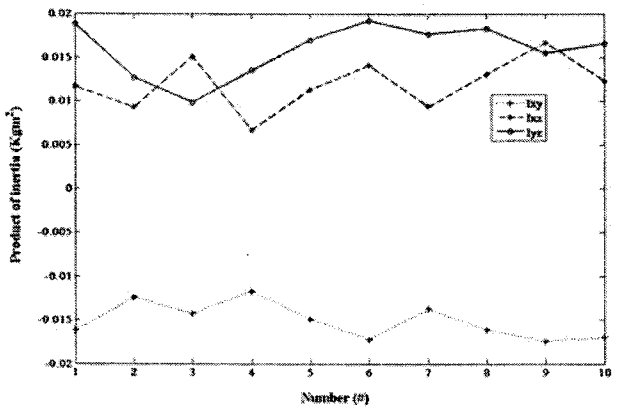

Figure 6. Product of inertia by experiments.

the desired orientation. The customized momentum wheel assemblies are developed for the simulator of ACL. Each of the momentum wheel assemblies is composed of a BLDC (Brushless Direct Current) motor, motor servo controller, and flywheel. First, the size of the flywheel, functioning as a torque generator, is calculated and estimated according to two versions. Second, on the basis of two kinds of flywheels (i.e., ver1-flywheel and ver2-flywheel), a test is performed to determine the proper range of torque generation. Third, in order to identify the performance of the servo controller that can control the momentum wheel assembly, a signal tracking test called a chirp test is performed. In identifying the primitive performance of each module and the characteristics of the finished product through experiments, these identifications can show what the performance of the integrated momentum wheel after integration. The verification of the changed specifications can be of further help in predicting the performance of the HIL simulator maneuvered by the momentum wheels.

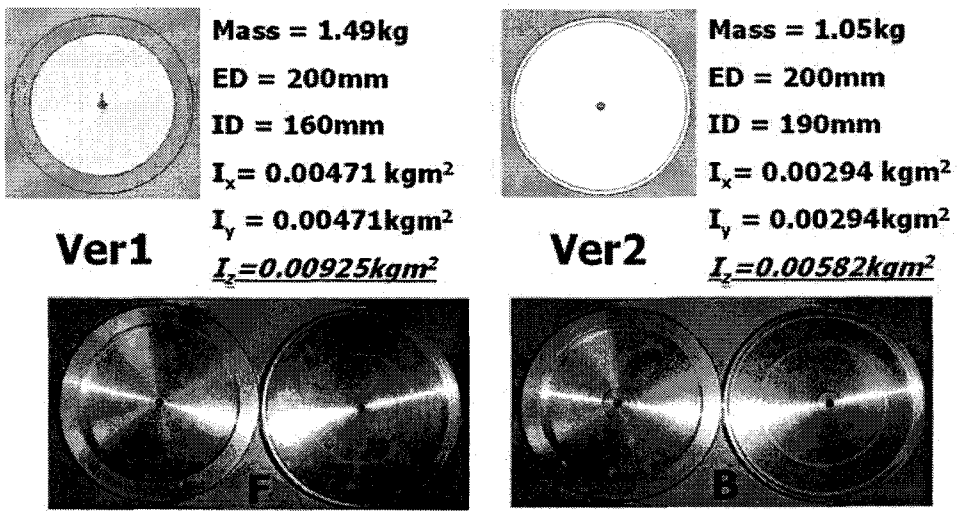

Figure 7. Dimensions and external shape of two types of flywheels (ver1 and ver2) (ED: Exterior diameter, ID: Interior diameter, I_x: x element of moment of inertia, I_y: y element of moment of inertia, I_z: z element of moment of inertia, F: Front of each flywheel, B: Back of each flywheel).

5.1 Flywheel sizing

The momentum wheel assembly (MWA) should have proper performance so that it orients the HIL simulator in the desired directions. On the basis of Euler equation (M (torque) $= I \cdot \alpha$), I (moment of inertia) and α (angular acceleration) of momentum wheel should be determined. However, it is not easy to determine the proper sizing because I and α are trade-off relations. Two types of flywheels with different moments of inertia I are used to identify what factor has greater influence on the production of torque. The most efficient way to design flywheel is one in which the mass is concentrated in its rim; in other words, the majority of the mass is located at the largest radius possible (Norton 2006). On the basis of the dimensions of initial sizing, moment of inertia is calculated according to flywheel versions. The mass moment of inertia of the flywheel is dependent on the specific geometry of the wheel and can be found by treating the disk and ring separately and superimposing the results. Figure 7 shows the specification of two types of flywheels.

5.2 Rotation frequency application to the momentum wheel

In order to test the customized momentum assembly as the essential component of the HIL simulator, input signals rapidly increasing with time are entered into the set value connector of the motor controller. According to the input of signals with high frequency, the performance of the motor controller can be confirmed. Such a frequency test is called a chirp test. A chirp is a signal in which the frequency increases ('up-chirp') or decreases ('down-chirp') with time. It is commonly used in sonar and radar, but has other applications, such as in spread spectrum communications. The reasons that the chirp test is applied to MWA as actuators are as follows: when the momentum wheel operates at the fastest speed according to the linear chirp waveform, the chirp test judges whether the motor servo controller can effectively process the input signal with the acceleration value despite a fast signal. The brushless DC motor used by the MWA of the HIL simulator can reach about

Table 2. The variations of rotational speed of the flywheels according to 10 cases α (angular acceleration).

Case (α)	1 (0.21)	2 (0.22)	3 (0.23)	4 (0.24)	5 (0.25)	6 (0.26)	7 (0.27)	8 (0.28)	9 (0.29)	10 (0.30)
Acc of Ver1. (rad/s^2)	12.762	13.294	13.500	13.770	14.093	14.276	14.331	14.563	14.568	14.763
Acc of Ver2. (rad/s^2)	18.994	19.349	19.832	19.841	20.440	20.451	20.713	20.778	21.221	21.293
Torque of Ver1. (kgm^{2}2/s^2)	0.118	0.123	0.125	0.127	0.130	0.132	0.133	0.135	0.135	0.137
Torque of Ver2. (kgm^2/s^2)	0.111	0.113	0.115	0.115	0.119	0.119	0.121	0.121	0.124	0.124

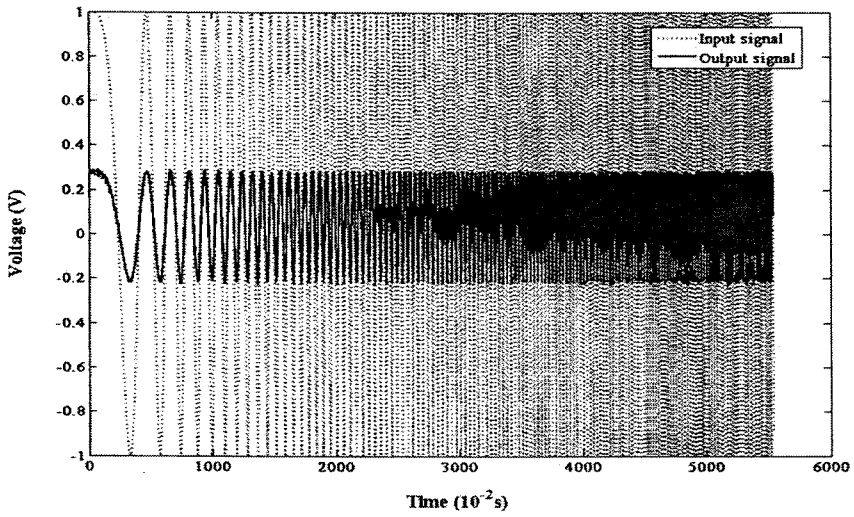

Figure 8. Comparison between input signal and output signal.

5,500 rpm (575.67 rad/s) in a power system environment of 12V input. Therefore, the rotation frequency according to the maximum speed is 91.67 Hz. The chirp test allows the momentum wheel to accelerate linearly to the target frequency of the maximum 91.67 Hz in 55 seconds.

6. Test Results for Momentum Wheels and Total Implementation

6.1 Ramp test (acceleration test for sizing the flywheel)

A flywheel is a rotating disk used as a storage device for kinetic energy. Flywheels resist changes in their rotational speed, which helps steady rotation of the shaft when a fluctuating torque is exerted on it by its power source. When a satellite receives any disturbance torque in a space environment, the MWA can offset the disturbance torque by operation of the momentum wheel. On the basis of the flywheels in Figure 7, acceleration tests according to each flywheel are performed. The object for the experiments is to identify how much torque two types of flywheels have and how quickly the momentum wheel displays the response. By linearly increasing 10 cases of α, the variations of flywheel speed are yielded, as seen in Table 2. The comparison result shows that the angular acceleration α of the ver2-Flywheel with a small Moment Of Inertia (MOI) is larger. The MOI rates

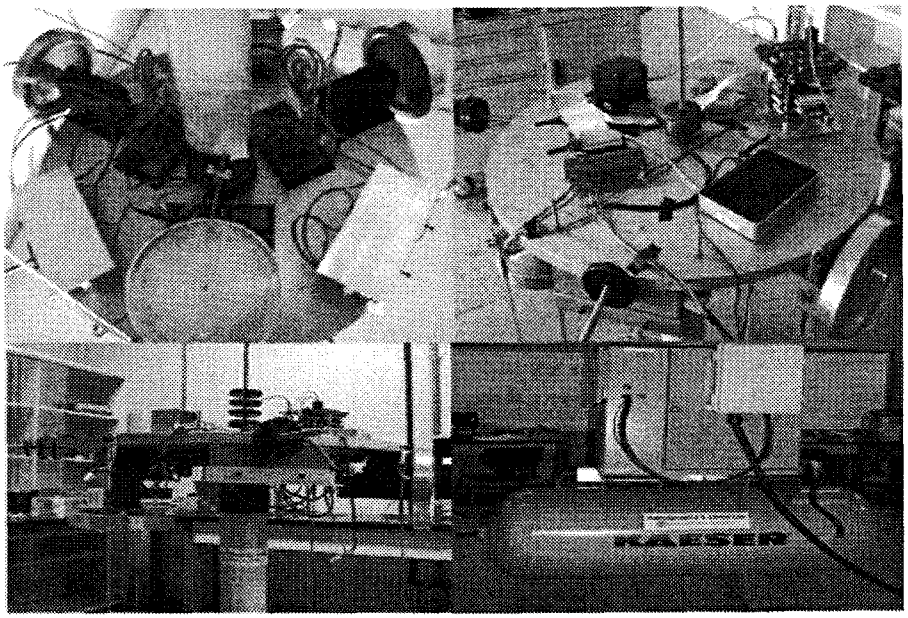

Figure 9. Real simulator (upper-left: bottom view, upper-right: top view, lower-left: side view, lower-right: an air compressor).

of the two types of flywheels are MOI of ver.2/MOI of ver.1=0.629. The increasing rate of α ((acc. of ver.2 - acc. of ver.1) / acc. of ver.1) according to the decrease of MOI is 0.451. This shows that the increasing width of α does not offset the decreasing rate of MOI and causes the difference of torque generated by two types of flywheels. The difference of average torque according to the two versions in 10 experiments is Avg. 0.0113 kgm^3/s^2. Through the ramp test, it is found that MOI has a greater influence on the quantity factor of torque. In other words, it will be effective to design a flywheel with a bigger MOI if greater torque is required. Thus, in the event of MWA including the version-2 flywheel with the smaller MOI, as provided in the figures, the momentum wheel displays more sensitive responses according to acceleration variations. That is, if a more agile response is required in the situation necessary for the identical torque, diminishing MOI compared to α can be helpful.

6.2 Chirp test (frequency test for identifying the signal tracking of motor servo controller)

The chirp test judges whether a motor servo controller can effectively process input signals with acceleration values or not. Test results from frequency increasing with time for input and output signals are shown in Figure 8. In Figure 8, the graph oscillating in the range of +/– 1.0 V is the input signal and the graph with oscillation in +/– 0.3 V is the output signal. In Figure 8, the input signal goes through aliasing because the signal has high frequency during a short period after about 5000 ms (sample time: 0.01 s). The figure shows that output follows input signal quite well, except for the aliasing part identified in the time domain for both phase and amplitude factor. This result can show a direct relation with the performance of the HIL simulator for spacecraft attitude control, in that the motor servo controller as a key part of momentum wheel assembly displays an excellent signal

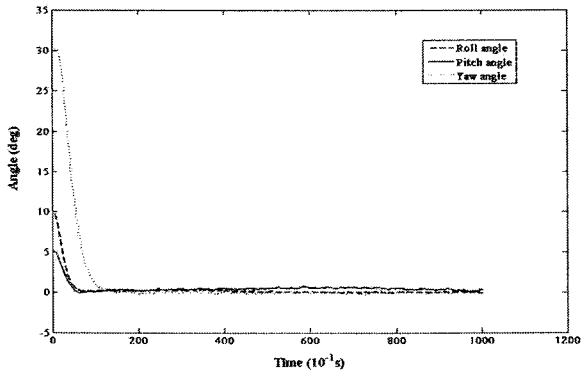

Figure 10. Experimental result when implementing PID controller (angle).

feedback.

6.3 PID implementation (integrated test for the HIL simulator)

Based on the two types of momentum wheel tests, the characteristics of the momentum wheels are identified and the test results influence total system operation and gain tuning of the controller since momentum wheels produce the torque that can allow the simulator to practically actuate itself. In this research, the PID controller takes charge of the control of the simulator. Figure 9 is an appearance set showing a real simulator which can show the performance of the simulator by applying the PID controller. MATLAB SIMULINK is used for both the entire system interface and the implementation of the PID controller. Passing by several gain tunings, the test results of the roll, pitch, and yaw axes display stable performance. With the estimated inertia of the HIL simulator, the control test results of the roll, pitch, and yaw axes reach stable performance. The experiments include the maneuver of 10 deg in the roll axis, the maneuver of 5 deg in the pitch axis, and the maneuver of 30 deg in the yaw axis. The settling time for reaching 5 % (maximum required accuracy: +/– 0.1 deg) of error is about 9 sec for the roll (10 deg) axis, about 6 sec for the pitch (5 deg) axis, and about 14 sec for the yaw (30 deg) axis, as can be seen in Figure 10. Figure 11 also shows that angular velocity reaches steady state response for all axes.

7. Conclusions

To simulate the spacecraft attitude system on the ground, an HIL simulator was developed. For the success of the frontier missions in the future, it is important not only to develop a control algorithm but also to validate the algorithm using a hardware system like the HIL simulator. With such an intention, this paper shows the characteristics of a low cost HIL simulator for spacecraft attitude control using momentum wheels. The HIL simulator used three customized momentum wheels designed and established for 3-axis control as actuators. The wheels were tested and proved by several experiments. In chirp test results, the output acceleration by momentum wheel successfully tracks the input acceleration by chirp. In the ramp test, applying two types of flywheels, the variation of moment of inertia affects the amount of output torque more, and a smaller moment of inertia enables the momentum wheel to control the simulator more sensitively. In order to verify the capability

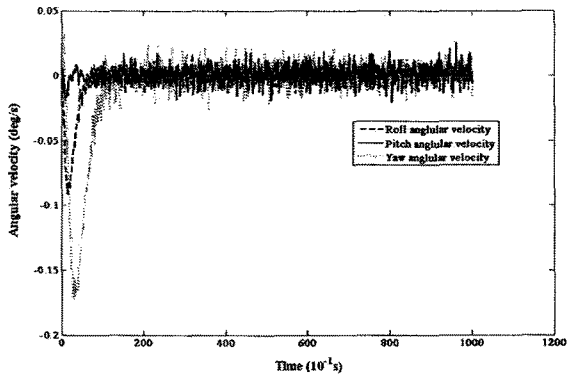

Figure 11. Experimental result when implementing PID controller (angular velocity).

of the developed HIL simulator, a PID controller is implemented, and the simulator shows a stable performance. The HIL simulator for spacecraft attitude control can perform the implementation of linear and nonlinear attitude controllers. Hence, the HIL simulator can be effectively used to validate the performance of innovative attitude control schemes and to enhance reliability of the schemes in real space missions. Furthermore, for educational purposes, the simulator can give assistance in improving learning and understanding, as students may visually grasp satellite systems and attitude control.

Acknowledgements: The author would like to acknowledge the Korean Science and Engineering Foundation (KOSEF) for financial and technical support for the National Research Laboratory (NRL) Project funded by the Ministry of Science and Technology (No. M10600000282-06J0000-28210).

References

Edwards, S., Lavagno, L., Lee, E. A., & Vincentelli, A. S. 1997, Proceedings of the IEEE, 85, 366

Kim, B. M., Velenis, E., Kriengsiri, P., & Tsiotras, P. 2001, AIAA/AAS Astrodynamics Specialists Conference, AIAA 2001-367

Kim, D. 2008, Master Thesis, Yonsei University

Norton, R. L. 2006, Machine Design: An integrated approach, 3rd Ed. (New Jersey: Prentice Hall)

Penrose, R. 1955, Proceedings of the Cambridge Philosophical Society, 51, 406

Schwartz, J. L., Peck, M. A., & Hall, C. D. 2003, JGCD, 26, 513

Tanygin, S. & Williams, T. 1997, JGCD, 20, 625

Wang, F., Cao, Xi-Bin, Yang, Y., & Gao, D. 2006, AIAA Modeling and Simulation Technologies Conference and Exhibit, AIAA 2006-6733